



# Preliminary Study of Blue Dye Removal on Small Sodium Alginate Hydrogel Beads in Fixed-Bed Glass Columns: A Basic Experimental and Mathematical Approach

Estudio preliminar de la eliminación de colorante azul en perlas pequeñas de hidrogel de alginato de sodio en columnas de vidrio de lecho fijo: Un enfoque experimental y matemático básico

Ana Pamela Fuerte Aguilar<sup>1</sup>, Brian Carlos Cerrito Florencio<sup>2</sup>, José Luis Zárate Castrejón<sup>3</sup>, Vicente Peña Caballero<sup>4\*</sup>

1-4 Universidad de Guanajuato, Campus Celaya-Salvatierra, DCSI, Departamento de Ingeniería Agroindustrial, Sede Mutualismo, Programa Educativo de Licenciatura en Ingeniería en Biotecnología. Sección de Análisis Dinámico de Bioprocesos, Laboratorio de Investigación en Biotecnología. Prolongación Río Lerma s/n, Col. Suiza, C.P. 38060
vicente.caballero@ugto.mx 4

#### **Abstract**

Bioadsorption within a packed-bed column is a bioprocess in which a continuous mass transfer occurs between two phases. In this preliminary study, the Bohart and Adams' model considering bed depth, and influent dye concentration was studied to exhibit adsorption process of blue dye in glass columns. The dynamic bed capacity and the adsorption rate constant values are determined using the Bohart and Adams' bed depth service model. Adsorption breakthrough curves were calculated as a function of C/C<sub>0</sub> vs time. Results showed that with the increases of bed height, and the decreases of influent dye concentrations, the breakthrough time was very similar for the four bed heights. The results demonstrated that SSAHB can be suggested as an adsorbent for removal of blue dye from wastewaters of industrial plants for the tertiary treatment of real liquid effluents,

**Keywords:** Adsorption on a fixed-bed column; blue dye, Adams-Bohart model, Small Sodium Alginate Hydrogel Beads.

#### Resumen

La bioadsorción en una columna de lecho fijo es un bioproceso en el que se produce una transferencia de masa continua entre dos fases. En esta investigación preliminar, se estudió el modelo de Bohart y Adams, que tiene en cuenta la profundidad del lecho y la concentración del colorante en la corriente de entrada para mostrar el proceso de adsorción del colorante azul en columnas de vidrio. La capacidad dinámica del lecho y los valores de la constante de velocidad de adsorción se determinaron utilizando el modelo de servicio de profundidad del lecho de Bohart y Adams. Las curvas de ruptura de la adsorción se calcularon con base a C/C<sub>0</sub> vs tiempo. Los resultados mostraron un aumento de la altura del lecho y la disminución de las concentraciones de colorante influyente, el tiempo de ruptura fue muy similar para las cuatro alturas del lecho. Los resultados demostraron que el PPHAS puede sugerirse como adsorbente para la eliminación del colorante azul de las aguas residuales de plantas industriales para el tratamiento terciario de efluentes líquidos reales.

Palabras clave: Adsorción en una columna de lecho fijo; colorante azul, modelo Adams-Bohart, pequeñas perlas de hidrogel de alginato de sodio.



# VOLUMEN 37 XXX Verano De la Ciencia ISSN 2395-9797

www. jovenesenlaciencia.ugto.mx

# **List of symbols (Nomenclature)**

$t_b$	Service time at breakthrough point (min)
-------	--

- $N_0$  The dynamic bed capacity (mg/L)
- z The packed-bed column depth (m)
- U The linear flow rate (m/min), defined as the ratio of the volumetric flow rate to the cross-sectional area of the bed
- $k_{ads}$  the adsorption rate constant (  $min/L \ min$  ).

- $Q_v$  Volumetric flow rate  $(m^3 / min)$
- $S_c$  The cross-sectional area of the bed  $(m^2)$ ,
- $C_0$  The inlet dye concentration (mg/L)
- $C_t$  The concentration of effluent at time (mg/L)
- $C_b$  The breakthrough metal ions concentration (mg/L)



# VOLUMEN 37 XXX Verano De la Ciencia ISSN 2395-9797

www.jovenesenlaciencia.ugto.mx

### Introduction

Environmental challenges in the modern era are intrinsically complex, often involving interrelated social, economic, and ecological dimensions. Among the most critically affected non-renewable resources is water, which faces increasing stress due to both domestic and industrial overexploitation and the resulting pollution. Water contamination has become a pressing global concern, driven by a network of interdependent factors that have collectively contributed to a worsening water crisis characterized by the depletion of groundwater reserves and the widespread discharge of untreated wastewater. Year after year, the agricultural sector remains the largest water consumer compared to other economic sectors, accounting for 32.2% of total water use in Mexico and approximately 72% globally. This is followed by the industrial and service sectors, which together consume 12.2% in Mexico and 15% and 13%, respectively, on a global scale (INEGI, 2025; UNESCO, 2025). However, water use also presents a secondary yet equally critical issue: the discharge of untreated wastewater originating from both domestic (municipal) and non-domestic (industrial) sources. According to recent reports by the United Nations (2023, 2024), it is estimated that 73% of industrial waste and 42% of domestic wastewater are inadequately treated or discharged without treatment. Therefore, the environmental impact of the industrial sector is not solely due to its water consumption, but rather its substantial contribution to water pollution.

Among the most environmentally burdensome industries, the textile sector stands out as one of the largest contributors to global pollution. It is estimated to be responsible for approximately 8% of global greenhouse gas emissions and consumes an estimated 215 billion liters of water annually (UN, 2025). Furthermore, it is the leading industrial source of synthetic dye contamination in wastewater, primarily due to the release of unfixed dyes during manufacturing processes (Pérez, 2024). The World Bank estimates that textile production accounts for roughly 20% of global water pollution, largely attributed to the dyeing stage of the textile manufacturing process. During this stage, between 10% and 25% of the dye fails to bind to textile fibers, and consequently, an estimated 16% of the initial dye load is directly discharged into wastewater streams (Khan, 2022).

Numerous studies have emphasized that synthetic dyes are highly ecotoxic compounds, typically classified based on the chemical structure of the chromophore group or application method (*Table 1*). Among them, azo and anthraquinone dyes are the most extensively used in the textile industry due to their structural versatility, strong affinity for a wide range of fibers, and compatibility with various dyeing techniques. Furthermore, the chemical interactions between dye molecules and textile fibers significantly influence their environmental release. For example, reactive dyes form covalent bonds with fibers, resulting in the generation of potentially hazardous products and conferring resistance to degradation. In contrast, disperse and direct dyes exhibit dissolution mechanisms that facilitate their mobility in aqueous effluents.

Particularly azo dyes, have been associated with adverse health effects, including mutagenicity and carcinogenicity, as well as environmental persistence due to their high chemical stability and resistance to biodegradation factors that contribute to their bioaccumulation and potential biomagnification in trophic chains. Moreover, these dyes are known to contribute to eutrophication processes, given the nitrogen containing functional groups within their chromophore structures, which can stimulate uncontrolled proliferation of plant tissue at the physiological level (Zaruma, 2018). Likewise, acid, direct, and sulfur dyes have shown elevated toxicity toward aquatic organisms and harmful effects on human health, particularly involving dermal and ocular exposure.

Table 1. Classification of Synthetic Dyes

Dye Type	Chromophore Groups	Application Method	Applications	Examples
Acid	Azo, anthraquinone, triphenylmethane, nitro, and nitroso	Applied in dye baths with neutral to acidic pH	Textiles, leather, pharmaceuticals	Acid Yellow 36, Acid Orange 7, Acid Blue 83
Basic	Azo, triphenylmethane, and anthraquinone	Applied in basic dye baths	Textiles, paper	Methylene Blue, Rhodamine 6G
Direct	Azo	Fiber immersion in an electrolyte-containing bath	Textiles	Direct Black 19, Direct Red 28, Direct Blue 86
Azo	Azo	Varies depending on fiber type	Textiles, paper, leather, cosmetics, food, pharmaceuticals	Rhodamine B, Acid Red 18, Methyl Orange, Methyl Red
Disperse	Azo, anthraquinone, nitro	Diffusion fixation at high temperature and pressure	Textiles, food, pharmaceuticals	Disperse Red 167, Disperse Blue 56, Disperse Yellow 211



# VOLUMEN 37 XXX Verano De la Ciencia ISSN 2395-9797

www. jovenesenlaciencia.ugto.mx

Nitro	Azo and anthraquinone	Applied in neutral dye baths with chromium salts	Textiles	Naphthol Yellow (II)
Reactive	Azo and anthraquinone	Covalent reaction with fiber depending on temperature and pH	Textiles	Reactive Red 120, Reactive Red 198
Sulfur	Indeterminate structures	Reductive application followed by oxidation	Textiles, paper	Sulfur Brilliant Green, Sulfur Blue, Sulfur Black 1, Ferric Anhydride
Mordant	Azo and anthraquinone	Use of mordants such as chromium salts	Textiles	Acid Yellow 36, Acid Orange 7, Acid Blue 83
Vat	Anthraquinone and indigo derivatives	Reduction with hydrosulfite followed by oxidation	Textiles	Methylene Blue, Rhodamine 6G

Source: Own Elaboration using data from Pérez et al. (2024) y Zaruma et al. (2018).

Ecosystems have exhibited extraordinary resilience in adapting to the presence of complex pollutants ranging from biological and physical to chemical and xenobiotic agents. Nevertheless, their regenerative capacity is increasingly compromised by the persistent exposure to and fluctuating composition of contaminated effluents (Bundschuh, 2023).

In this context, the development and continuous refinement of wastewater treatment technologies remain imperative to mitigate the environmental discharge of toxic substances into aquatic and terrestrial ecosystems. Numerous studies have assessed the potential of various treatment strategies such as membrane separation, coagulation—flocculation, adsorption, precipitation, ion exchange, and bioremediation for the removal of synthetic dyes from wastewater streams (Rendón, 2024). Each of these approaches presents inherent limitations concerning efficiency, operational cost, scalability, and suitability under diverse environmental conditions (Khan, 2022). Among them, adsorption has emerged as a particularly promising technique due to its high removal efficiency at low contaminant concentrations, operational simplicity, cost-effectiveness, and the feasibility of utilizing low-cost, reusable, or waste-derived adsorbents (e.g., valorized agro-industrial residues). When compared to other technologies, fixed-bed column adsorption offers additional advantages such as ease of scale-up, process continuity, and the absence of secondary pollutant generation, making it a sustainable and robust alternative for real-world applications (Patel, 2019).

A wide range of mathematical models has been developed to simulate and predict the performance of adsorption systems. Nonetheless, experimental validation remains indispensable for fine-tuning design and operational parameters, particularly when transitioning from laboratory-scale setups to industrial-scale implementations. Kinetic evaluation of the adsorbent–adsorbate interactions enable the determination of critical operational metrics (including breakthrough time, saturation time, adsorption capacity, and rate constants) which are essential for predicting system behavior under dynamic conditions and for optimizing adsorbent performance and process economics.

Among the available modeling approaches, simplified kinetic models such as the Thomas, Yoon–Nelson, and Bed Depth Service Time (BDST) models are widely adopted in fixed-bed column studies. While these models neglect the effect of intraparticle diffusion (a significant internal mass transfer resistance) they are still considered robust, as they assume that external film diffusion and surface reaction kinetics govern the overall adsorption process. Their simplicity reduces mathematical complexity while retaining predictive accuracy and practical relevance (Patel, 2019).

Conventional adsorption studies are often conducted in batch systems, wherein a fixed amount of adsorbent is exposed to a known contaminant concentration until equilibrium is reached. However, fixed-bed column adsorption operates under continuous-flow conditions, establishing a dynamic mass transfer regime between the liquid phase (adsorbate) and the solid phase (adsorbent bed). This configuration not only provides a more realistic approximation of industrial wastewater treatment processes but also facilitates the monitoring of adsorption dynamics in real-time. During column operation, the mass transfer zone progresses along the bed until the adsorbent becomes saturated. Thereafter, the concentration of the target contaminant in the effluent rises until it stabilizes at the influent concentration. In adsorption kinetics, a key operational benchmark is the breakthrough time defined as the point at which the effluent concentration reaches 10% of the influent level. This behavior is typically illustrated via a breakthrough curve, plotting the dimensionless concentration ratio  $(C/C_0)$  against time. These curves serve as essential tools for characterizing system performance under varying operational conditions.



This study aimed to evaluate the performance of a continuous adsorption system using a fixed-bed column (packed bed) under diverse experimental settings. Specifically, the influence of initial dye concentration, volumetric flow rate, and bed height on removal efficiency was investigated.

### Materials, methods, and instrumentation

### Small sodium alginate hydrogel beads preparation

Calcium alginate method (Ruiz-Marin et al., 2010; Siripattanakul and Khan, 2010) was used to prepare small sodium alginate (SA) hydrogel beads (SSAHB) with an average spherical diameter of 1 mm. SSAHB were made by dripping the SA (3% *w/v*) into 4% (*w/v*) sterile calcium chloride solution. The Ca<sup>2+</sup> plays a key role in the cross-linking of the alginate polymer to form a solid bead. After overnight hardening, SSAHB of diameter 0.5–1 mm were formed and then rinsed with sterilized and distilled water.

#### Alginate solution preparation

Sodium alginate solution (4% w/v) was made by incrementally adding sodium salt of alginate into beakers containing distilled water. An overhead mechanical stirrer was placed over the beaker; initial rotation was set to 100 rpm which was gradually increased by  $\approx$  100 rpm with each added aliquot of sodium alginate. It was essential to stir the final mixture overnight ( $\approx$ 350 rpm) to achieve complete dissolution (i.e., viscous, clear solution) (P.U. Ashvin et al., 2024).

#### Comment (instrumentation)

The formation of the SSAHB was produced by dripping the SA into sterile calcium chloride solution applying a centrifugal force with a new system designed by 3D printing, which is in the process of intellectual property protection, for which reason no further details of the developed system are given. But if it is of academic or research interest, you can request support to the E-mail: vicente.caballero@ugto.mx, jl.zarate@ugto.mx.

#### Sorption Test

The sorption experiment was carried out in a four-column fixed bed system with SSAHB for different bed height z (0.138, 0.3144, 0.438 and 0.548 m) as shown in Figure 1 (experimental scheme of column study). In addition, the fixed parameters used were 5 ppm inlet concentration of blue commercial dye  $C_0$  (El Caballito®), the liquid flow  $Q_v$  (1.0 and 1.5 L/min) controlled by a peristaltic pump (Masterflex L/S, Model 7523-90 by Col-Parmer) using Cole-Parmer Masterflex Multichannel 4-Ch Peristaltic Pump 7523-80 & Head 7536-04 (see Figure 1 for three analysis factors: inflow, initial concentration and bed height. According to this preliminary study), and the system was run at temperature  $\approx 27^{\circ}C$ .

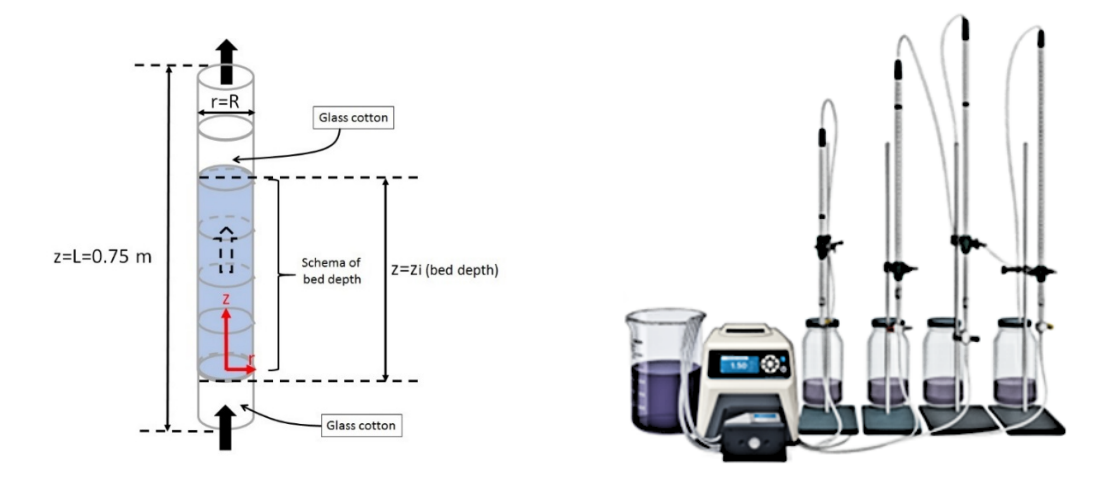


Figura 1. Experimental setup of the fixed-bed column system. Image generated from photographs using Illustrae.co software. Source: Own elaboration (left) using Illustrae.co software (right).



# ISSN 2395-9797

www.jovenesenlaciencia.ugto.mx

Adsorption Test (Adsorption modeling)

The model employed was Adams-Bohart model, different parameters were derived from model which described the performance of the adsorption column. The linear and nonlinear adsorption model is described as follows.

$$\frac{C_t}{C_0} = \frac{1}{1 + e^{\left(\frac{k_{ads}zN_0}{U} - k_{ads}C_0t\right)}}$$
(1a)

or

$$y = \frac{1}{1 + e^{[k_{ads}(a - bx)]}}$$
 (1b)

Where  $a = \frac{zN_0}{U}$ ,  $b = C_0$ ,  $y = \frac{C_t}{C_0}$ , and x = t

Now, for simplicity, the linear version of the nonlinear model in equation (2) is as follows:

$$ln\left(\frac{C_0}{C_b} - 1\right) = ln\left(e^{\left(k_{ads}N_0\left(\frac{z}{U}\right)\right)} - 1\right) - k_{ads}C_0t_b \tag{2}$$

Where  $t_b$  is the service time at breakthrough point (min),  $N_0$ the dynamic bed capacity (mg/L), z the packed-bed column depth (m), U: the linear flow rate (m/min) defined as the ratio of the volumetric flow rate  $Q_v$  (m³/min), to the cross-sectional area of the bed  $S_c$  (m²),  $C_0$  and  $C_b$  are, respectively, the inlet and the breakthrough metal ions concentration (mg/L) and  $k_{ads}$  the adsorption rate constant (min/L min). Equation (2) known under the name of bed depth service time (BDST) can be determined for a given adsorbent depth and is a straight line (Hutchins, 1973):

$$\underbrace{t_{b_i} = \left[\frac{N_0}{C_0 U}\right] z_i - \left[\frac{1}{k_{ads} C_0}\right] ln\left(\frac{C_0}{C_b} - 1\right)}_{inear\ relation\ between \ the\ column\ bed\ depth\ (z)} \rightarrow \underbrace{y_i = \beta_0 + \beta_1 x_i; i = 1, 2, ..., n}_{Bed\ height\ versus\ time} : \Rightarrow \begin{cases} y_i = t_{b_i} \\ \beta_0 = \left[\frac{1}{k_{ads} C_0}\right] ln\left(\frac{C_0}{C_b} - 1\right) \\ \beta_1 = \left[\frac{N_0}{C_0 U}\right] \\ x_i = z_i \end{cases}$$

$$(3)$$

Equation (3) is satisfied if it is verified in Equation (2) that:  $e^{\left(k_{ads}N_0\left(\frac{z}{\overline{U}}\right)\right)}\gg 1$  thus  $ln\left(e^{\left(k_{ads}N_0\left(\frac{z}{\overline{U}}\right)\right)}-1\right)\cong 0$ 

 $k_{ads}N_0\left(\frac{z}{U}\right)$ . Then, from Equations (3),  $\beta_0(min)$  and  $\beta_1(min\,m^{-1})$ , respectively, is the slope of the BDST line and represents the time required for the adsorption zone to travel a unit length through the adsorbent and is the abscissa intercept in the BDST plot and the dynamic bed capacity ( $N_0$ ) and the adsorption rate constant ( $k_{ads}$ ) can be evaluated from the slope and intercept of the plot of  $t_b$  versus  $z_i$ :  $N_0 = \beta_1 C_0 U$  and  $k_{ads} = \left[\frac{1}{\beta_0 c_0}\right] ln\left(\frac{c_0}{c_b} - 1\right)$  (see Appendix A: a fast algorithm to solve systems of linear equations, i.e, Equation (2)).

**Remark** ( $z_{i=0} = z_0$ ). The bed depth ( $z_0$ ), which represents the theoretical depth of SSAHB able to prevent the adsorbent concentration from exceeding  $C_b$ , is obtained when  $t_b = 0$  (see Equation (3)), according to the following equation:

$$0 = \left[\frac{N_0}{C_0 U}\right] z_0 - \left[\frac{1}{k_{ads} C_0}\right] ln\left(\frac{C_0}{C_b} - 1\right) \rightarrow z_0 = \left[\frac{U}{N_0 k_{ads}}\right] ln\left(\frac{C_0}{C_b} - 1\right)$$
 (3)

The reader is referred to paper Patel, eta al. (2019) for further details of models available in the literature for linear modeling of packed bed columns or design of the adsorption column based on bed depth service time.



### Results and discussions

Small sodium alginate hydrogel beads preparation

Figure 2 presents a brief size comparison at both macroscopic and microscopic (5x) scales of the sodium alginate (3%) hydrogels generated using a traditional dripping method with a syringe, and those employed as the adsorbent medium in the present study.

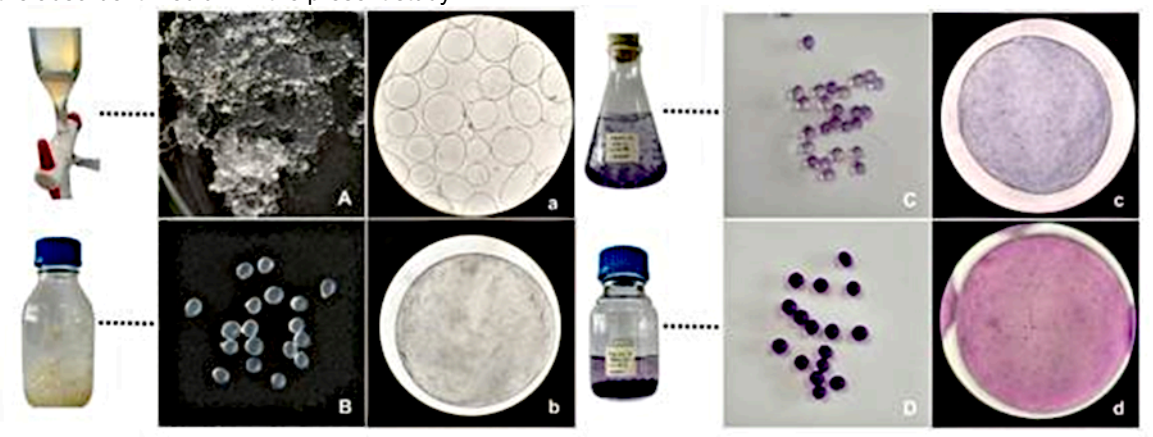


Figura 2. Macroscopic and microscopic (5×) view of sodium alginate hydrogels.

NOTE: On the left side (uppercase labels), the general morphology is shown; on the right side (lowercase labels), the surface structure is depicted under optical microscopy. Samples A and B correspond to hydrogels not exposed to the contaminant, whereas C and D show hydrogels subjected to different dye concentrations (20 and 100 mg/L, respectively) to assess their behavior under batch adsorption conditions. Source: Own elaboration.

The initial column system design (*Figure 3*) served as a preliminary setup for the final experimental trials due to several technical constraints. Notably, significant challenges were encountered in introducing and removing the hydrogel adsorbent, primarily due to air entrapment and limited outlet flow caused by the narrow internal diameters at both ends of the column. Furthermore, inconsistencies in the internal diameter across different columns introduced experimental variability, preventing accurate comparative analysis. This geometric heterogeneity led to non-uniform flow distribution and residence time, thereby influencing the mass transfer dynamics within the bed.



Figura 3. Initial design scheme of the column system. Source: Own elaboration using Illustrae.co software.

Additional limitations arose from the use of commercial textile dyes, which typically incorporate various additives that compromise chemical purity—unlike analytical-grade reagents. In the textile industry, mordants or fixing agents are often added to enhance dye adherence to fabrics. The dye utilized in this study (El Caballito®) exemplifies such formulations, containing an integrated fixative. While this may represent a competitive advantage in industrial applications, it introduces significant analytical challenges in laboratory





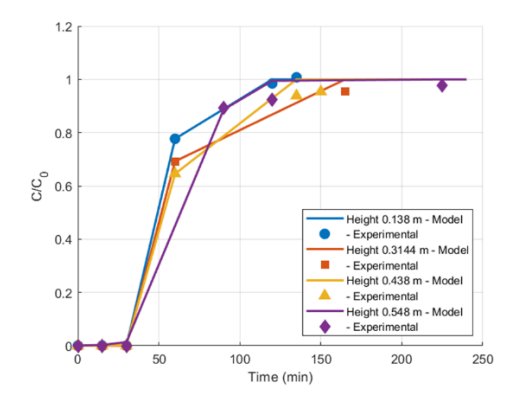
settings. The presence of the fixative may interfere with spectrophotometric measurements and adversely affect gravimetric dosing accuracy.

This complication stems from the heterogeneous composition of the dye product, where the colorant and fixative components exhibit variable particle sizes and are not uniformly blended. Moreover, the manufacturer does not disclose the chemical composition of either the dye or the fixative, further limiting experimental control and reproducibility. As a result, during weighing procedures, the precise amount of actual dye versus additive remains uncertain—an issue that becomes critically important when working at low concentrations (ppm), as is the case in the present study. This factor must be carefully considered during the generation of the dye calibration curve, as the contribution of the fixative to the overall absorbance cannot be ruled out. One possible mitigation strategy is the acquisition of dye standards from the PUTNAM® fixed-dye product line, which excludes fixatives from its formulation. Alternatively, the experimental uncertainty introduced by the fixative can be minimized through particle size screening or sieving prior to use.

#### Column studies

Effect of bed depth and inlet concentration

The breakthrough curves obtained for blue dye adsorption are demonstrated in Figure 4 for different bed depth of SSAHB (0.138, 0.3144, 0.438 and 0.548 m), at a constant flow rate of 1.0 and 1.5 mL/min.



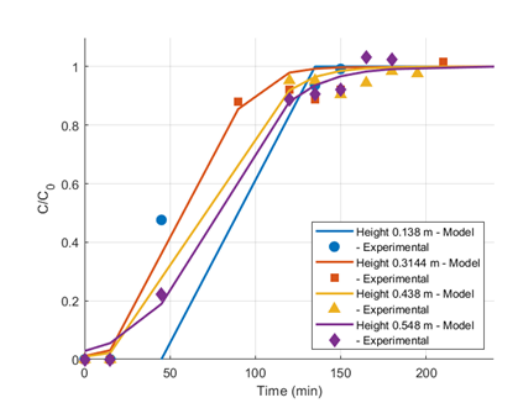


Figura 4. Break point curves of blue dye at various flow rates and bed depth: (right) Qv = 1.0 mL/min (left) Qv = 1.5 mL/min. Source: Own elaboration.

To calculate the model parameters  $N_0=\beta_1C_0U$  and  $k_{ads}=\left[\frac{1}{\beta_0c_0}\right]\ln\left(\frac{c_0}{c_b}-1\right)$  of Equation (1), the model is linearized (Equation (2)) and for two linear feed flows to the columns (Q<sub>v</sub>:1.0 and 1.5 mL/min) and four different bed depth (z: 0.138, 0.3144, 0.438 and 0.548 m) (see *Figure 5*). The solid line corresponds to the model in Equation (3) for each flow in the columns and the markers for each  $t_b$  and  $C_b$ .

With the values of the parameters  $N_0$  and  $k_{ads}$  (results not shown here with the correlation coefficients for the plots were in the range 0.9656-0.9675 in Figure 5) the values of these parameters are calculated by nonlinear fitting using the Excel solver based on Equation (1b). The results for the parameter a are presented in Tables 2 and 3. and then the values of the parameters  $k_{ads}$  and  $N_0$  in Table 4. According to the results for  $k_{ads}$  and  $N_0$ , the estimated values of the variable  $y = \frac{C_{\rm t}}{C_0}$  (see Equation (1b)) are shown in the solid lines and the experimental observations (markers) in Figures 4. Results show that an increase in slope when the inlet dye concentration decreases ( $C_0$ = 8.176 to  $C_0$ = 7.92), allowing to treat a larger volume of solution with increase in  $Q_v$ . These results are consistent with the results reported by Patel, et al. (2019) and P.U. Ashvin Iresh et al., (2014).

The results demonstrated that SSAHB could be suggested as an adsorbent for removal of blue dye from wastewaters of industrial plants for the tertiary treatment of real liquid effluents.



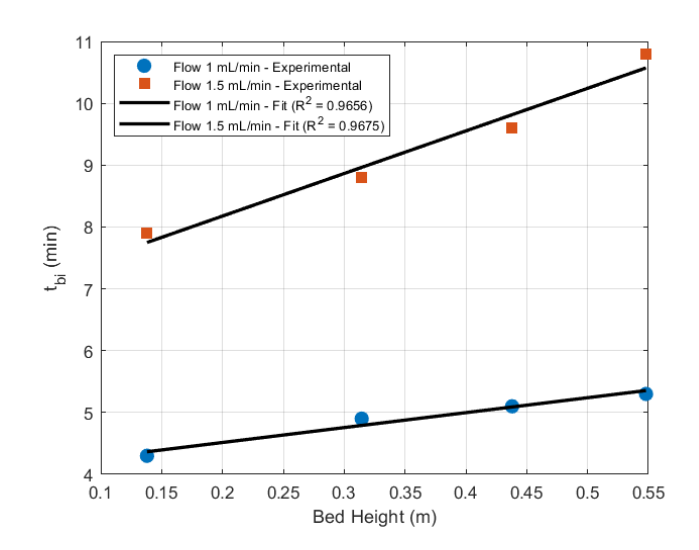


Figura 5. The breakthrough times depend on bed depth for blue dye. Source: Own elaboration

Table 2. Parametres calculated used for the flow 1 mL/min.

Flow: 1 $\frac{mL}{min}$ , b= $C_0$ = 8.176 $\frac{mg}{L}$ (see Equation (1b))			
z (m)	$U\left(\frac{m}{min}\right)$	$a\left(\frac{mg \cdot min}{L}\right)$	
0.138	0.010997	458.95	
0.3144	0.012602	470.0197	
0.438	0.011682	469.182	
0.548	0.010904	576.9402	

Source: Own elaboration

*Table 3.* Parametres calculated used for the flow 1.5 mL/min.

Flow: 1.5 $\frac{mL}{min}$ , b= $C_0 = 7.92 \frac{mg}{L}$ (see Equation (1b))			
Z (m)	$U\left(\frac{m}{min}\right)$	$a\left(\frac{mg \cdot min}{L}\right)$	
0.138	0.0165	753	
0.3144	0.0189	511	
0.438	0.0175	626	
0.548	0.0164	607	

Source: Own elaboration

www.jovenesenlaciencia.ugto.mx

**Table 4.** Model parameters calculated for flow (ml/min) and bed depth (m), applicated the nonlinear equation adsorption model

Z (m)	Flow: 1 $\frac{mL}{min'}$ , b= $C_0$ = 8.176 $\frac{mg}{L}$ (see Equation (1b))		Flow: 1.5 $\frac{m}{m}$ (see E	Flow: 1.5 $\frac{mL}{min}$ , b= $C_0 = 7.92 \frac{mg}{L}$ (see Equation (1b))	
	$N_0(\frac{mg}{L})$	$k_{ads}(\frac{min}{mg\ L})$	$N_0(\frac{mg}{L})$	$k_{ads}(\frac{min}{mg\ L})$	
0.138	0.217	0.039	0.019	1.407	
0.3144	0.249	0.034	1.030	0.009	
0.438	0.231	0.028	0.956	0.007	
0.548	0.215	0.013	0.892	0.006	

Source: Own elaboration

#### **Conclusions**

First, to produce very small alginate beads, a mold was designed and printed on a 3D printer. The complete system for forming the beads is in the process of intellectual property protection. In addition, the present study has shown that the textile blue dye can be removed by adsorption onto the small sodium alginate (SA) hydrogel beads (SSAHB). The BDST model was successfully used to analyze column performance and evaluate the model parameters. Nowadays software is available to analyze the dynamic response of adsorption processes, e.g., Aspen Adsorption, however in this work a mathematical and numerical analysis was carried out using the models from their mathematical basis as it was a summer course with the participation of students in training process has potential applicability for the removal of dyes generated by the textile industry, whose residues may reach drinking water sources or contribute to environmental pollution. SSAHB can be suggested as an adsorbent for removal of blue dye from wastewaters of industrial plants for the tertiary treatment of real liquid effluents. Finally, the characterization of the adsorbents (SSAHB) was reserved for another publication.

# **Declaration of competing interests**

The authors declare that they have no known competing financial interests or personal relationships that could have appeared to influence the work reported in this paper.

# Data availability

Supporting Information associated with to the development of numerical codes can be requested via E-mail: vicente.caballero@ugto.mx, and jl.zarate@ugto.mx.

# Acknowledgements

This research is partially supported by: Verano de la Ciencia XXX (Diseño de sistemas de adsorción de metales en fase acuosa a base de residuos agroindustriales) and proyecto de investigación de la convocatoria institucional de investigación científica 2024": ciic 2024-fortalecimiento de la capacidad académica de la Universidad de Guanajuato (UG) (estudio de adsorción en fase acuosa a régimen lote y continuo en lecho fijo utilizando substratos agotados de cultivos de *Pleurotus djamor* como adsorbentes de cr(VI)) for the availability of the equipment financed by this project, which was the basis for the development of the research. Finally, at the Rectoría del Campus Celaya-Salvatierra (CCS) of the UG and the División de Ciencias de la Salud (DSCI) and to the Secretaría de Ciencia, Humanidades, Tecnología e Innovación (Secihti) for the call for proposals (CBF-2025-G-1840).

#### References

Ashvin Iresh Fernando, P. U., Kennedy, A. J., Pokrzywinski, K., Jernberg, J., Thornell, T., George, G., Kosgei, G. K., Wang,



# **VOLUMEN 37** XXX Verano De la Ciencia

ISSN 2395-9797

www.jovenesenlaciencia.ugto.mx

- Y., & Coyne, K. J. (2024). Development of alginate beads for precise environmental release applications: A design of experiment based approach and analysis. Journal of Environmental Management, 351, 119872. https://doi.org/10.1016/j.jenvman.2023.119872
- Belter, P. A., Cussler, E. L., & Hu, W.-S. (1988). Bioseparations: Downstream processing for biotechnology. John Wiley & Sons.
- Bohart, G. S., & Adams, E. Q. (1920). Adsorption in columns. Journal of the American Chemical Society, 42(3), 523-544.
- Bundschuh, M., Mesquita-Joanes, F., Rico, A., & Camacho, A. (2023). Understanding ecological complexity in a chemical stress context: A reflection on recolonization, recovery, and adaptation of aquatic populations and communities. Environmental Toxicology and Chemistry, 42(9), 1857-1866.
- Edgar, T.F, & D.M. Himmelblau. (1988). Optimization of Chemical Processes. New York: McGraw-Hill.
- González-Delgado, A., Tejada-Tovar, C., Villabona-Ortiz, A., Vergara-Villadiego, J., & Olivella-Henao, E. (2022). Modelado y parametrización de una columna de adsorción para la remoción de níquel utilizando ingeniería de procesos asistida por computador. Revista EIA, 21(42), 1-18. https://doi.org/10.24050/reia.v21i42.1778
- Hutchins, R. A. (1973). New method simplifies design of activated carbon systems. American Institute of Chemical Engineers Journal, 80(4), 133-138.
- Instituto Nacional de Estadística y Geografía. (2025, 19 de marzo). Estadísticas a propósito del Día Mundial del Agua (Comunicado de prensa Núm. 51/25). INEGI. https://www.inegi.org.mx/contenidos/saladeprensa/aproposito/2025/EAP\_DMunAgua.pdf
- Khan, A. A., Gul, J., Naqvi, S. R., Ali, I., Farooq, W., Liaqat, R., AlMohamadi, H., Štěpanec, L., & Juchelková, D. (2022). Recent progress in microalgae-derived biochar for the treatment of textile industry wastewater. Chemosphere, 306, 135565. https://doi.org/10.1016/j.chemosphere.2022.135565
- Mohammad, H., Hanafy, H., & Hassan, H. (2014). Remediation of lead by pretreated red algae: adsorption isotherm, kinetic, column modeling and simulation studies. Green Chemistry Letters and Reviews, 7(4), 342-358.
- Noticias ONU. (2025, 29 de marzo). La moda rápida alimenta la crisis mundial de los residuos. Naciones Unidas. https://news.un.org/es/story/2025/03/1537631
- Organización de las Naciones Unidas. (2023). Blueprint for acceleration: Sustainable Development Goal 6 synthesis report on water and sanitation 2023 (pp. 9-33). https://www.unwater.org/publications/sdg-6-synthesis-report-2023
- Organización las Naciones Unidas. (2024).Un-Water Annual Report 2024. https://www.unwater.org/sites/default/files/2025-06/un-water annualreport 2024 25june2025.pdf
- Patel, H. (2019). Fixed-bed column adsorption study: A comprehensive review. Applied Water Science, 9(45). https://doi.org/10.1007/s13201-019-0927-7
- Pérez Ramírez, E. E., de la Luz Asunción, M., Martínez-Hernández, A. L., Méndez Lozano, N., & Velasco Santos, C. (2024). Los nanomateriales de carbono: una alternativa prometedora para la remoción de colorantes del agua mediante adsorción. Tendencias en Energías Renovables V Sustentabilidad, https://doi.org/10.56845/terys.v3i1.220
- Rendón Castrillón, L., Ramírez Carmona, M., Ocampo López, C., González-López, F., Cuartas Uribe, B., & Mendoza Roca, J. A. (2024). Efficient bioremediation of indigo-dye contaminated textile wastewater using native microorganisms combined bioaugmentation-biostimulation techniques. Chemosphere. https://doi.org/10.1016/j.chemosphere.2024.141538
- Ruiz-Marin, A., Mendoza-Espinosa, L. G., & Stephenson, T. (2010). Growth and nutrient removal in free and immobilized green algae in batch and semi-continuous cultures treating real wastewater. Bioresource Technology, 101, 58-
- Singh, S. K., Dhruv, K., Mehta, D., & Sehgal, D. (2015). Fixed bed column study and adsorption modelling on the adsorption of malachite green dye from wastewater using acid activated sawdust. International Journal of Advanced Research, 3(7), 521-529.
- Siripattanakul, S., & Khan, E. (2010). Fundamentals and applications of entrapped cell bioaugmentation for contaminant removal. In V. Shah (Ed.), Emerging environmental technologies (pp. 147-169). Springer.
- United Nations Educational, Scientific and Cultural Organization. (2025). The United Nations World Water Development Report 2025: Mountains and glaciers: water towers (pp. 9-10). https://doi.org/10.54679/LHPJ5153
- Zaruma, P., Proal, J., Hernández, I. C., & Salas, H. I. (2018). Los colorantes textiles industriales y tratamientos óptimos de sus efluentes de agua residual: una breve revisión. Revista de la Facultad de Ciencias Químicas, 19, 38-47.



# Appendix A. A fast algorithm to solve systems of linear equations

Solution for the equation of a line using matrix-vector notation

To solve the parameters ( $\beta_0$  and  $\beta_1$ ) of the equation of the reactive line model,

$$\hat{y}_i = \beta_0 + \beta_1 x_i; i = 1, 2, ..., n$$
 (A1)

 $\hat{y}_i = \beta_0 + \beta_1 x_i; \ i=1,2,\dots,n \quad (A1$  Which can be written in matrix-vector from for n data points (experimental data  $P_i(x_i,\hat{y}_i)$ ), as:

$$\begin{bmatrix} \hat{y}_1 \\ \hat{y}_2 \\ \vdots \\ \hat{y}_n \end{bmatrix} = \begin{bmatrix} x_1 & 1 \\ x_2 & 1 \\ \vdots & \vdots \\ x_n & 1 \end{bmatrix} \underbrace{\begin{bmatrix} \beta_0 \\ \beta_1 \end{bmatrix}}_{parameter\ of\ model} \rightarrow \hat{Y} = X \underbrace{\theta}_{parameter\ of\ model}$$
(A2)

Where  $\hat{\mathbf{Y}} \in \mathbb{R}^{n \times 1}$ ;  $\mathbf{X} \in \mathbb{R}^{n \times 2}$  and  $\boldsymbol{\theta} \in \mathbb{R}^{2 \times 1}$ . Then, the objective function is:

$$f(\theta) = \sum_{i=1}^{n} (y_i - \hat{y}_i)^2 = [Y - \hat{Y}]^T [Y - \hat{Y}] : subject to \hat{Y} = X\theta \quad (A3)$$

Where  $f(\theta) \in \Re^{1 \times 1}$ ,  $\left[ Y - \widehat{Y} \right]^T \in \Re^{1 \times n}$  and  $\left[ Y - \widehat{Y} \right] \in \Re^{n \times 1}$ . The solution is (Edgar and Himmelblau, 1988):

 $\boldsymbol{\theta} = (\boldsymbol{X}^T \boldsymbol{X})^{-1} \boldsymbol{X}^T \boldsymbol{Y} = \begin{bmatrix} \beta_0 \\ \beta_1 \end{bmatrix} \Rightarrow MatLab \ rutines \ polyfit \ and \ polyval:$ 

Remark (see equation (2)).  $\boldsymbol{\theta} = colum[\beta_0 \quad \beta_0] = colum\left[\left[\frac{1}{k_{ads}C_0}\right]ln\left(\frac{C_0}{C_h}-1\right) \quad \frac{N_0}{C_0U}\right] \rightarrow \text{paremeter of model}$ (Equation A1)

 $\theta = polyfit(x, y, 1)$  and  $\hat{Y} = polyval(\theta, x)$ 

Remark. Fit Nonlinear Bohart Adams Model in Originpro

$$\mathbf{X}^{T}\mathbf{X} = \begin{bmatrix} x_{1} & x_{2} & \cdots & x_{n} \\ 1 & 1 & \cdots & 1 \end{bmatrix} \begin{bmatrix} x_{1} & 1 \\ x_{2} & 1 \\ \vdots & \vdots \\ x_{n} & 1 \end{bmatrix} \equiv \begin{bmatrix} \sum_{i=1}^{n} x_{i}^{2} & \sum_{i=1}^{n} x_{i} \\ \sum_{i=1}^{n} x_{i} & n \end{bmatrix}$$
(A4)

$$\boldsymbol{X}^{T}\boldsymbol{Y} = \begin{bmatrix} x_{1} & x_{2} & \cdots & x_{n} \\ 1 & 1 & \cdots & 1 \end{bmatrix} \begin{bmatrix} \hat{y}_{1} \\ \hat{y}_{2} \\ \vdots \\ \hat{y}_{n} \end{bmatrix} \equiv \begin{bmatrix} \sum_{i=1}^{n} x_{i} \hat{y}_{i} \\ \sum_{i=1}^{n} y_{i} \end{bmatrix}$$
 (A5)